A MODEL STUDY OF THE NOCTURNAL BOUNDARY LAYER

Li Xingsheng (李兴生) and *Yang Shuowen* (杨硕文)

Institute of Atmospheric Physics, Academia Sinica, Beijing

Received January 16, 1985

ABSTRACT

In this paper, a second-order model is proposed for the study of the evolution of the nocturnal boundary layer (NBL). The model is tested against the Wangara data on atmospheric boundary layer. The computer results show that the model can simulate some important characters observed in the NBL, and that a kind of sudden change may occur in the developing process of NBL.

I. INTRODUCTION

The K model is often utilized in simulating the structure of atmospheric boundary layer. With this kind of model many investigators, including Estoque[1] (1963), Sasamori[2] (1970) and Clarke[3] (1974), have made and discussed the numerical simulations of diurnally varying planetary boundary layer. On the other hand, Buajitti and Blackadar[4] (1957), Paegle and Rash[5] (1973) and Li et al.[6] (1980) have made similar models concentrating on the mechanism of formation of the low-level jet and the inversion in the NBL, and have discussed the relations between these phenomena and other factors. Although the K model can realistically simulate certain features observed in the planetary boundary layer, the determination of the K values is rather arbitrary, and the calculated turbulent fluxes are rather inaccurate.

In the latest decade some investigators have further discussed the structure of the planetary boundary layer with high-order models. This kind of model, such as that used by Yammada et al.[7] (1975), Wyngaard [8] (1975) and Andre et al.[9] (1978), can well simulate the mean quantities and the second moments, but Wyngaard's model did not include the influence of infra-radiation on the NBL. Although the model adopted by Andre et al. had higher orders, their simulation of the third moments remains to be discussed further. In this paper, a second-order model will be considered, and used to simulate the structure of the NBL of the Wangara area and discuss a kind of sudden change in the developing process of NBL.

II. THE MODEL

By assuming that the NBL is homogeneous in the horizontal plane, its mean structure only depends on time t and the altitude z. The meteorological variables to be considered are wind components $\bar{u}_i = (\bar{u}, \bar{v}, 0)$, potential temperature $\bar{\theta}$ and mixing ratio of water vapor $\bar{q}$.

In the following study the Boussinesq approximation is incorporated. The equations for mean quantities are

$$\frac{\partial \bar{u}}{\partial t} = f(\bar{v} - v_g) - \frac{\partial \overline{u'w'}}{\partial z}, \tag{1}$$

$$\frac{\partial \bar{v}}{\partial t} = -f(\bar{u} - u_g) - \frac{\partial \overline{v'w'}}{\partial z}, \tag{2}$$

$$\frac{\partial \bar{\theta}}{\partial t} = -\frac{\partial}{\partial z}\overline{w'\theta'} - \frac{1}{c_p \rho_0}\frac{\partial}{\partial z}(\bar{F}\uparrow - \bar{F}\downarrow), \tag{3}$$

$$\frac{\partial q}{\partial t} = -\frac{\partial}{\partial z}\overline{w'q'}, \tag{4}$$

where u_g and v_g represent eastward and northward components of geostrophic wind, f is the Coriolis parameter, $\bar{F}\uparrow$ and $\bar{F}\downarrow$ represent upward and downward mean long-wave radiative fluxes. The radiative fluxes are calculated with a method similar to that of Garret et al. [10](1981) as follows

$$\bar{F}\downarrow(z) = \int_0^{u_{top}-u(z)} B(\bar{T})\frac{d\varepsilon_d(u')}{du'}du' + \bar{F}\downarrow_{top}[\varepsilon_d(u_\infty - u) - \varepsilon_d(u_{top} - u)]/\varepsilon_d(u_\infty - u_{top}), \tag{5}$$

$$\bar{F}\uparrow(z) = \int_0^{u(z)} B(\bar{T})\frac{d\varepsilon_u(u')}{du'}du' + [1-\varepsilon_u(u)][\varepsilon_g B(\bar{T}_g) + (1-\varepsilon_g)\bar{F}\downarrow(0)], \tag{6}$$

where u is the mean amount of water vapor (g cm^{-1}) from the earth's surface to the altitude z, $u_{top}=u(z_{top})$, $\bar{F}\downarrow_{top}=F(z_{top})$, $u_\infty=u(\infty)$, z_{top} is the top height of the model, $B(\bar{T})$ is the emission of blackbody of temperature $\bar{T}$, ε_d and ε_u are the downward and upward emissivities given by the formulas suggested by Rodgers[11] (1967).

The governing equations for the second-order moments are

$$\frac{\partial}{\partial t}\overline{u_i'u_k'} + \overline{u_k'u_j'}\frac{\partial \bar{u}_i}{\partial x_j} + \overline{u_i'u_j'}\frac{\partial \bar{u}_k}{\partial x_j} + \frac{\partial}{\partial x_j}\overline{u_i'u_j'u_k'} = -\frac{1}{\rho_0}\left(\overline{u_k'\frac{\partial p'}{\partial x_i}} + \overline{u_i'\frac{\partial p'}{\partial x_k}}\right) + \frac{g}{\bar{\theta}}(\overline{u_k'\theta'}\delta_{3i} + \overline{u_i'\theta'}\delta_{3k}) - \frac{2}{3}\bar{\varepsilon}_e\delta_{ik} - 2\omega\varepsilon_{ijl}\eta_j\overline{u_l'u_k'} - 2\omega\varepsilon_{klm}\eta_l\overline{u_m'u_i'}, \tag{7}$$

$$\frac{\partial}{\partial t}\overline{\theta'^2} + 2\overline{\theta'u_j'}\frac{\partial \bar{\theta}}{\partial x_j} + \frac{\partial}{\partial x_j}\overline{u_j'\theta'^2} = -2\bar{\varepsilon}_\theta - 2\overline{\theta' C_R'}/C_p\rho_0, \tag{8}$$

$$\frac{\partial}{\partial t}\overline{\theta'u_i'} + \bar{\theta}\overline{u_j'}\frac{\partial \bar{u}_i}{\partial x_j} + \overline{u_i'u_j'}\frac{\partial \bar{\theta}}{\partial x_j} + \frac{\partial}{\partial x_j}\overline{\theta'u_i'u_j'} = -\frac{\overline{\theta'\frac{\partial p'}{\partial x_i}}}{\rho_0} + \frac{g}{\bar{\theta}}\overline{\theta'^2}\delta_{3i} - 2\omega\varepsilon_{ijk}\eta_j\overline{u_k'\theta'}, \tag{9}$$

$$\frac{\partial}{\partial t}\overline{q'\theta'} + \bar{\theta}'\overline{u_j'}\frac{\partial q}{\partial x_j} + \overline{q'u_j'}\frac{\partial \bar{\theta}}{\partial x_j} = -\bar{\varepsilon}_{q\theta}, \tag{10}$$

$$\frac{\partial}{\partial t}\overline{q'^2}+\overline{2q'u_j'}\frac{\partial \bar{q}}{\partial x_j}+\frac{\partial}{\partial x_j}\overline{q'^2u_j'}=-2\bar{\varepsilon}_q, \tag{11}$$

$$\frac{\partial}{\partial t}\overline{q'u_i'}+\overline{q'u_j'}\frac{\partial \bar{u}_i}{\partial x_j}+\overline{u_i'u_j'}\frac{\partial \bar{q}}{\partial x_j}+\frac{\partial}{\partial x_j}\overline{u_i'u_j'q'}$$

$$=-\frac{\overline{q'}\,\overline{\partial p'}}{\rho_0\partial x_i}+\frac{g}{\bar{\theta}}\overline{\theta'q'}\delta_{3i}-2\omega\varepsilon_{ikl}\eta_k\overline{u_j'q'}, \tag{12}$$

where g, ρ_0, p are the acceleration of gravity, the standard values of air density and the pressure, respectively; $\bar{\varepsilon}_e$, $\bar{\varepsilon}_\theta$, $\bar{\varepsilon}_{q\theta}$, $\bar{\varepsilon}_q$ are the molecular dissipations of the mean fluctuating kinetic energy $\bar{e}=\frac{1}{2}\overline{u_i'u_i'}$, the temperature variance $\overline{\theta'^2}$, the correlation moment $\overline{q'\theta'}$ between q and θ, and the mixing ratio variance $\overline{q'^2}$, respectively; ω is the earth rotation rate, η_i is the unit vector along the earth rotation axis. Summation should be made from 1 to 3 over subscripts which are repeated within a single term.

In Eqs. (7)—(12), we have assumed that the molecular dissipation is isotropic and the molecular diffusion fluxes are neglected. On the basis of dimensional analysis, we parameterize the molecular dissipation rates as follows

$$\bar{\varepsilon}_e=C_1(l)\bar{e}^{3/2}/l, \tag{13}$$

$$\left.\begin{aligned}\bar{\varepsilon}_\theta&=C_2\bar{\varepsilon}_e\bar{e}^{-1}\overline{\theta'^2},\\ \bar{\varepsilon}_q&=C_q\bar{\varepsilon}_e\bar{e}^{-1}\overline{q'^2},\\ \bar{\varepsilon}_{q\theta}&=C_{q\theta}\bar{\varepsilon}_e\bar{e}^{-1}\overline{q'\theta'},\end{aligned}\right\} \tag{14}$$

where parameters $C_2=0.8$, $C_q=C_{q\theta}=4.85$. The value of C_2 is deduced from the similarity law for stable stratification, and close to the value 0.7 utilized by Wyngaard[4]. The characteristic length l and parameter C_1 (l) are chosen in the way similar to that of Andre et al.[9] as follows

$$l=\mathrm{Min}(l_s,l_b), \tag{15a}$$

where l_s is the characteristic length for neutral and unstable stratifications

$$\left.\begin{aligned}l_s&=kz/(1+kz/l_0),\quad k=0.35,\\ l_0&=0.1\int_0^\infty \bar{e}^{1/2}z\mathrm{d}z/\int_0^\infty \bar{e}^{(1/2)}\mathrm{d}z,\end{aligned}\right\} \tag{15b}$$

and l_b is the permissible largest characteristic length in the stable stratification

$$l_b=0.75\bar{e}^{(1/2)}\left(\frac{g}{\bar{\theta}}\frac{\partial\bar{\theta}}{\partial z}\right)^{-\frac{1}{2}}, \tag{15c}$$

$C_1(l)$ is given by

$$C_1(l)=0.02+0.12l/l_s, \tag{15d}$$

where the sum 0.14 of the two numerical values is set according to the similarity law for the neutral surface layer limit.

The pressure terms which appear in Eqs. (7), (9) and (12) are parameterized by a way similar to that of Launder[12,13] (1975), i. e.,

$$-\frac{1}{\rho_0}\left(\overline{u_k'\frac{\partial p'}{\partial x_i}}+\overline{u_i'\frac{\partial p'}{\partial x_k}}\right)=-C_3\bar{\varepsilon}_e\bar{e}^{-1}\left(\overline{u_i'u_k'}-\frac{2}{3}\delta_{ik}\bar{e}\right)$$

$$-C_4\left(P_{ik}-\frac{2}{3}\delta_{ik}P\right), \tag{16}$$

$$-\frac{1}{\rho_0}\overline{\frac{\partial p'}{\partial x_i}\theta'} = -C_5\bar{\varepsilon}_e\bar{e}^{-1}\overline{\theta' u_i'} - C_6 P_{i\theta}, \tag{17}$$

$$-\frac{1}{\rho_0}\overline{\frac{\partial p'}{\partial x_i}q'} = -C_7\bar{\varepsilon}_e\bar{e}^{-1}\overline{q' u_i'} - C_8 P_{iq}, \tag{18}$$

where P_{ik} and P are the generation rates of Reynold stresses $\overline{u_i' u_k'}$ and the eddy kinetic energy, respectively. For the horizontal homogeneous fields

$$P_{ik} = \frac{g}{\bar{\theta}}(\overline{u_i'\theta'}\,\delta_{3k} + \overline{u_k'\theta'}\,\delta_{3i}) - \left(\overline{u_i' u_3'}\frac{\partial \bar{u}_k}{\partial x_3} + \overline{u_k' u_3'}\frac{\partial \bar{u}_i}{\partial x_3}\right),$$

$$P = \frac{g}{\bar{\theta}}\overline{w'\theta'} - \overline{u'w'}\frac{\partial \bar{u}}{\partial z} - \overline{v'w'}\frac{\partial \bar{v}}{\partial z},$$

while $P_{i\theta}$, P_{iq} are parts of the generation rates of heat fluxes $\overline{u_i'\theta'}$ and mixing ratio fluxes $\overline{u_i' q'}$, respectively

$$P_{i\theta} = \frac{g}{\bar{\theta}}\overline{\theta'^2}\delta_{3i} - \overline{\theta' u_j'}\frac{\partial \bar{u}_i}{\partial x_j},$$

$$P_{iq} = \frac{g}{\bar{\theta}}\overline{q'\theta'}\,\delta_{3i} - \overline{q' u_j'}\frac{\partial \bar{u}_i}{\partial x_j}.$$

In Eqs. (16)—(18), $C_3=5.5$, $C_4=0$, $C_5=4.85$, which are adjusted on the basis of similarity law. We use $C_6=0.5$ as suggested by Launder, $C_7=4.85$, $C_8=0.5$.

In this paper, the terms related to the third-order moments which appear in Eqs. (7)—(9), (11) and (12) are neglected. The measurements by Wyngaard and Cote[14] indicate that they are negligible in the surface layer in the stable stratification.

The term $-\frac{2\overline{\theta' C_R'}}{C_p\rho_0}$ in Eq. (8) represents the influence of radiation on the temperature variance. Approximately we use

$$-\frac{2\overline{\theta' C_R'}}{C_p\rho_0} = -\beta_\theta\overline{\theta'^2}. \tag{19a}$$

This formula was introduced by Twensend[15] (1958), and the parameter β_θ is set by

$$\beta_\theta = 0.1\bar{q}. \tag{19b}$$

As Brost and Wyngaard[16] (1978) did, we ignore the Coriolis terms in comparison to other terms. For example, in the equation for $\overline{u'w'}$, the ratio of the Coriolis term to the shear production term is of the order fl/u_*. In the stable stratification $u_*\sim 0.1$ m s^{-1}, $l\sim 10$ m, and $f\sim 10^{-4}$s^{-1} (middle latitude), we find $fl/u_* = 5\times 10^{-3}$.

III. NUMERICAL SCHEME AND ITS BOUNDARY AND INITIAL CONDITIONS

1. *Numerical Scheme*

In general, Eqs. (1)—(4) and the parameterized Eqs. (7)—(12) can be expressed as

$$\frac{\partial A_i}{\partial t} = -C_i'\bar{e}^{-1}\bar{\varepsilon}_e A_i + F(A_1, A_2, \cdots, A_{i-1}, A_{i+1}, \cdots, A_{19}, z), \tag{20}$$

where A_i ($i=1$—19) stands for any one of the quantities to be solved in Eqs. (1)—(4).

and (7)—(12), and constant $C_i' \geqslant 0$. The time finite-difference version of Eq. (20) is given by

$$A_i^{(n+1)} - A_i^{(n)} = -C_i' \Delta t (\bar{e}^{-1}\bar{\varepsilon}_*)^{(n)} A_i^{(n+1)} + \Delta t F(A_1^{(n)}, A_2^{(n)}, \cdots, A_{i-1}^{(n)}, A_{i-1}^{(n)}, \cdots, A_{19}^{(n)}, z), \tag{21}$$

where Δt is the time step, taking $\Delta t = 2s$, and $A_i^{(n)}$ represents the value of A_i at the nth step. The altitude z is transformed into ξ, a new coordinate, through the following relation

$$\xi = 0.0369z + 0.667 \ln\left(\frac{z}{0.01} + 1\right), \tag{22}$$

where z is measured in m. From Eq. (22) we obtain

$$\frac{\partial A_i}{\partial z} = \left(\frac{\partial A_i}{\partial \xi}\right)\left(\frac{d\xi}{dz}\right).$$

In the coordinate ξ the space finite-difference equivalent to Eq. (21) is erected with constant increments. A staggered grid system is used to calculate the first-order correlations at odd levels and the second-order ones at even levels. We use 40 odd levels, corresponding to the calculation thickness of 2 km

2. *Boundary Conditions*

(1) Lower boundary conditions

$$\bar{u} = \bar{v} = 0, \quad \bar{q} = \bar{q}(t),$$
$$\bar{\theta} \approx \bar{T}_g(t), \quad \text{for} \quad z = z_0,$$

where z_0 is the roughness of the surface, $z_0 = 1$ cm. The ground temperature $\bar{T}_g$ is calculated from the surface energy budget, i. e.,

$$\varepsilon_g \bar{F}\downarrow(0) - C_p \rho_0 \overline{w'\theta_0'} - \varepsilon_g B(\bar{T}_g) + G_0 - L\rho_0 \overline{w'q'} = 0, \tag{23}$$

where $G_0 = \lambda_s \left(\frac{\partial T_s}{\partial \eta}\right)_{\eta=0}$ is the upward heat flux at surface from the sublayer soil. As $L\rho_0 \overline{w'q'}$ in Eq. (23) is about one tenth of $\rho_0 C_p \overline{w'\theta_0'}$ in the case our model being applied to, it can be neglected. The soil temperature T_s is predicted by the thermal diffusion equation, i. e.,

$$\frac{\partial T_s}{\partial t} = a_s \frac{\partial^2 T_s}{\partial \eta^2} \tag{24}$$

We assume that the soil temperature remains constant at the 1 m depth. Upon making the transformation of coordinate $\eta' = \sqrt{\eta}$ and dividing η' into 10 identical sublayers, we calculate T_s with an explicit scheme.

At $z = z_2$, the second-order moments are calculated with Eqs. (7)—(12), and the partial derivatives of first-order moments with respect to space are given by the ones at $z = z_0$ and z_3 according to logarithm law i. e., for $z = z_2$,

$$\frac{\partial}{\partial z}\begin{pmatrix} \bar{u} \\ \bar{v} \\ \bar{\theta} \\ \bar{q} \end{pmatrix} = \frac{1}{kz_2}\begin{pmatrix} u_* \cos\alpha \\ v_* \sin\alpha \\ \theta_* \\ q_* \end{pmatrix} = \frac{1}{z_2 \ln(z_3/z_0)}\begin{pmatrix} \bar{u}(z_3) \\ \bar{v}(z_3) \\ \bar{\theta}(z_3) - \bar{\theta}(z_0) \\ \bar{q}(z_3) - \bar{q}(z_0) \end{pmatrix} \tag{25}$$

(2) Upper boundary conditions

The second-order correlations and the gradients of the vertical fluxes are zero, and the mean quantities can be predicted by their governing equations with turbulent terms being zero.

3. *Initial Conditions*

The initial values for wind, temperature and mixing ratio are observed values, from which we first calculate the friction velocity u_*, characteristic temperature $\theta_*(=-\overline{w'\theta'_0}/u_*)$ and Monin-Obukhov length L according to the similarity law, then the second-order moments related to velocity and temperature. Let the absolute values of these moments decrease linearly from ground to the 500 m altitude, and remain small constants between 500-2000 m. The initial values for $\overline{w'q'}$, $\overline{q'\theta'}$ and $\overline{q'^2}$ are zero.

The formulas of similarity law mentioned above are

$$\overline{u'_s w'} = -u_*^2,\quad \overline{v'_s w'} = \overline{u'_s v'_s} = 0;\quad \overline{w'\theta'_0} = Q_0,$$

$$\overline{\theta'^2}\,(u_*^2/Q_0^2) = \begin{cases} 4(1-8.3\zeta)^{-2/3}, & \zeta<0, \\ 4, & \zeta>0, \end{cases}$$

$$\overline{v'_s\theta'} = 0;\quad \overline{u'_s\theta'}/Q_0 = \begin{cases} -3.7(1-15\zeta)^{-1/4}(1-9\zeta)^{-1/2}, & \zeta<0, \\ -3 & \zeta>0, \end{cases}$$

$$\overline{u'^2_s} = \begin{cases} 4u_*^2+0.3w_*^2, & Q_0>0, \\ 4u_*^2 & Q_0<0, \end{cases}$$

$$\overline{v'^2_s} = \begin{cases} 1.75u_*^2+0.3w_*^2, & Q_0>0, \\ 1.75u_*^2 & Q_0<0, \end{cases}$$

$$\overline{w'^2} = \begin{cases} [1.75+2(-\zeta)^{2/3}]u_*^2, & \zeta<0 \\ 1.75u_*^2, & \zeta>0 \end{cases}$$

$$\zeta = z/L.$$

IV. RESULTS

The simulations are compared with the data of Wangara atmospheric boundary layer[11] in the period of 33th day 18 hr through 34th day 06 hr. The geostrophic wind is deduced from observed data, i. e., first, linearly interpolate the surface values of geostrophic wind components and the values of thermal wind in terms of time, then, based on the values obtained above, utilize parabolic profiles to estimate the geostrophic wind components $u_g(z,t)$, $v_g(z,t)$.

1. *The First-Order Moments*

The computed and observed values of wind speed $V_h=(\bar{u}^2+\bar{v}^2)^{1/2}$ are shown in Fig. 1, where it can be seen that the computed results comparatively tally with the observed. After midnight the low-level jet appears and at 03 hr it has a maximum. On the other hand, the computed values are slightly less than the observed, which is probably due to the neglect of advection in the model and/or to the underestimation of values of geostrophic wind.

Fig. 2 compares the calculated with the observed profiles of mean temperature. It can be seen in the Fig. 2 that, on the whole, they have the same developing trend, but the computed thickness of inversion is a little less than the observed, and the computed intensity of inversion larger than the observed. The cause for this difference may be that the computed mixing ratio in the vicinity of the top of inversion is less than the observed, and the computed radiative cooling rate is underestimated. In addition, this may be attributed partly to the neglect of advection in the model.

The relations of inversion thickness, its intensity (the temperature difference between inversion top and ground), and the height, at which the wind maximum occurs, to the geostrophic wind are discussed in the paper. The results show that if the initial values of all quantities are in neutral equilibrium state and other external conditions maintain unchanged, then providing the geostrophic wind (being constant in every case) is adjusted from 5 m s^{-1} to 10 m s^{-1}, the inversion thickness and the wind-maximum-occurring height increase by a factor of about 3, and the intensity of inversion decreases nearly by 50 %. Li et al.[6] have also obtained similar results through forcing the cooling rate of the ground. The alternation of geostrophic wind, as we know, means the variation of diurnally averaged wind speed. Hence, if we want to model the evolution of NBL fairly well, the wind and its varying process should be simulated with quite high accuracy.

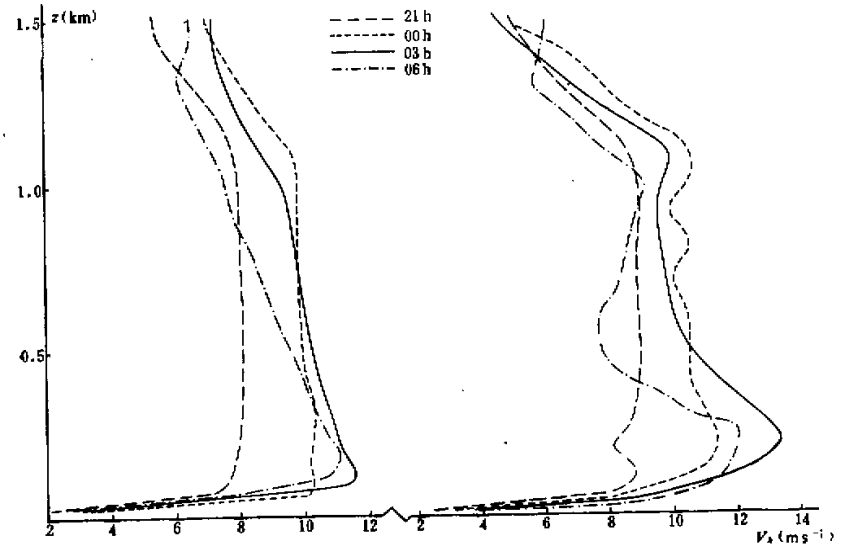

Fig. 1. The computed (left) and observed (right) values of wind speed.

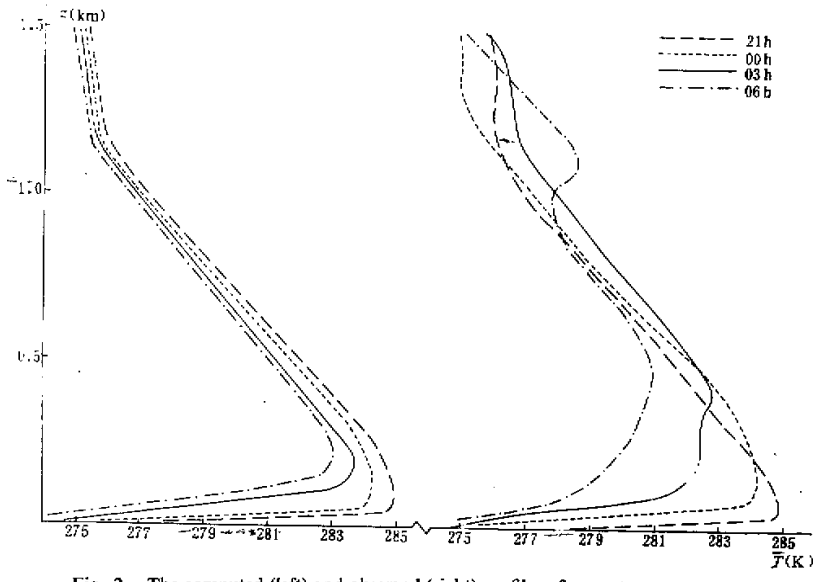

Fig. 2. The computed (left) and observed (right) profiles of mean temperature.

2. *The Second-Order Correlations*

Fig. 3 shows the profiles of computed mean eddy kinetic energy $\bar{e}$. Owing to the interaction of wind field with temperature field, $\bar{e}$ is very large in the surface layer with large shear of wind, and close to zero in the vicinity of inversion top with relatively small shear of wind. At higher levels $\bar{e}$ increases by a little, then decreases to zero.

The computed profiles of Reynold stresses $\overline{u'w'}$ and $\overline{v'w'}$ are presented in Fig. 4. Comparing Figs. 3 with 4, one can notice that $|\overline{u'w'}|$ and $|\overline{v'w'}|$ have nearly the same distribution as $\bar{e}$. The comparison between Figs. 4 and 1(left) shows that after 0 hr the low-level jet occurs in the inversion top with small Reynold stress. The computed results show that the Reynold stress is negligible as comparing with Coriolis force, therefore, the occurrence of lowlevel jet is due to the mechanism similar to the free-inertial oscillation pointed out by Blackadar[13] (1957).

3. *The Phenomenon of Sudden Change*

In this paper, a kind of sudden change occurring in the NBL is simulated. After the advent of the sudden change, the turbulent intensity fluctuates within a wide range, the wind velocity and temperature also change more rapidly at this time than the other time.

The evolutions of the computed mean fluctuating kinetic energy $\bar{e}$ and the turbulent heating rate $-\dfrac{\partial\overline{w'\theta'}}{\partial z}$ are shown in Fig. 5. One can see that $\bar{e}$ and $-\dfrac{\partial\overline{w'\theta'}}{\partial z}$ may vary within a large scope in a short time, and decay in a quasi-periodic way with time. The computed results show that the other second-order correlations also undergo similar processes.

It can also be seen in Fig. 5a that the sudden change spreads from the upper layer to the lower layer. The sudden change is thought to have resulted from the interaction between wind field and temperature field, whereas the quasi-periodic variations are probably due to the self-adjustment of turbulent fields. The computed results with the altered time step (being minified by 20 times) have no obvious difference from that computed with $\Delta t = 2s$. This verifies that the computed sudden change is not due to the numerical instability in computing process.

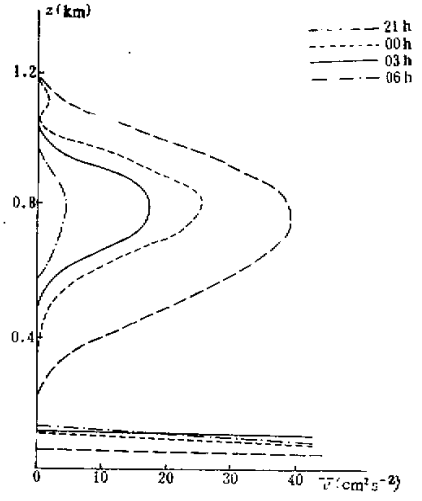

Fig. 3. The profiles of computed mean eddy kinetic energy. $\bar{e}$ measured in $cm^2\ s^{-2}$.

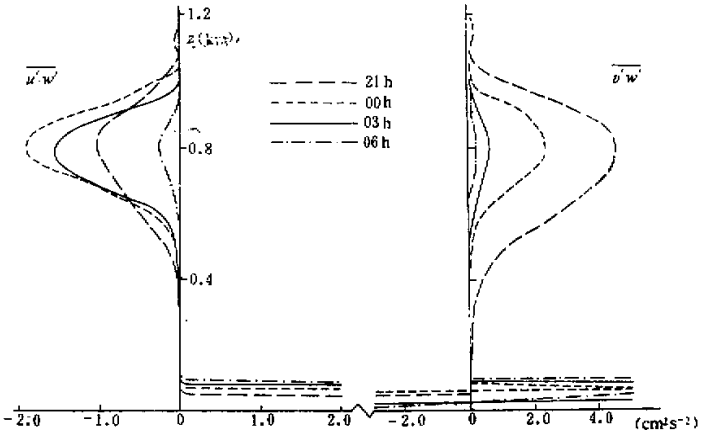

Fig. 4. The computed profiles of Reynold stresses $\overline{u'w'}$ (left) and $\overline{v'w'}$ (right).

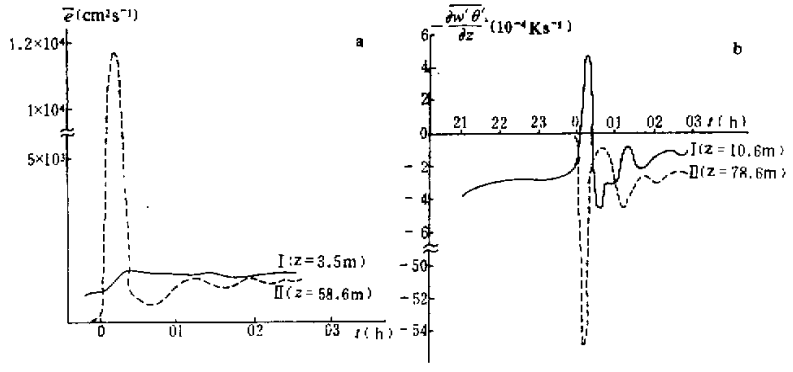

Fig. 5. The evolution of computed mean flactuating kinetic energy $\bar{e}$ (left) and turbulent heating rate $-(\partial\overline{w'\theta'})/\partial z$ (right).

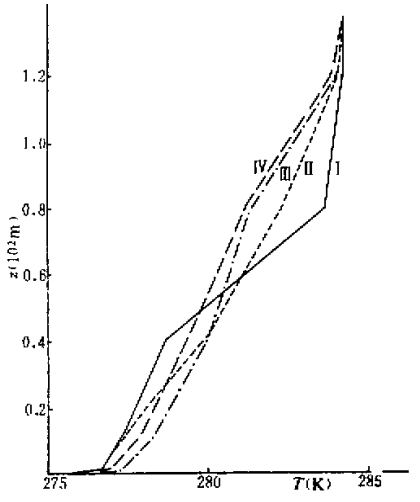

Fig. 6. The profiles of mean temperature before and after the occurrence of sudden change. Profiles I at 00:00, II 00:10, III 00:20, and IV 00:40.

The profiles of mean temperature before and after the occurrence of sudden change are presented in Fig. 6. It can be seen that after the sudden change takes place, the temperature rises within a relatively wide range in the lower layer, and falls considerably in the layer where the sudden change first occurs, which is consistent with the results shown in Fig. 5b. Here, the computed varying extent and rate of temperature are of the same

order as that observed by Zhou et al.[19] (1982) in the stable stratification, and the computed tendency of the temperature variation also resembles their observations to a certain extent.

Shown in Fig. 7 are the computed curves of intensity of wind shear $S_v=\left(\frac{\partial \bar{u}}{\partial z}\right)^2+\left(\frac{\partial \bar{v}}{\partial z}\right)^2$ and Richardson number $R_i=\frac{g}{\bar{\theta}}\frac{\partial \bar{\theta}}{\partial z}\Big/S_v$ in the layer where sudden change first occurs. One can see that, after the sudden change crops up, the intensity of wind shear decreases very rapidly, while Richardson number grows much fast as a result of turbulent mixing. Later, both quasi-periodically decay to stable values. The computed results show that the characteristic length of energy-containing eddies in the sudden change first-occurring layer is about 15 m, and the minimum mean kinetic energy is about 10^{-5} cm^2 s^{-2} (3 hr before the occurrance of sudden change). Therefore, let $l=15$ m, $\bar{e}=10^{-5}$cm^2 s^{-2} at initial time, $\overline{w'^2}=\frac{2}{3}\bar{e}$ and other second-order correlations be zero, we simulate the evolutions of $\bar{e}$ and other second-order moments with Eqs. (7)—(12) at different values of intensity of wind shear and Richardson number. The computed curves of the evolution of $\bar{e}$ at different values of S_v and at $Ri=0.3$ are presented in Fig. 8. We can see that the equilibrium of $\bar{e}$ under the condition of $S_v=1\times10^{-2}$ s^{-2} is of the same order as the maximum value of $\bar{e}$ in Fig. 5a, and at that time $S_v=2.1\times10^{-2}$s^{-2} (see Fig. 7). This means that it is possible for maximum value of $\bar{e}$ to appear in the sudden change, and also we can see that $\bar{e}$ varies rapidly before reaching its equilibrium value. Therefore, the above-computed sudden change is possible too.

It can be seen in Fig. 8 that the time for $\bar{e}$ to reach a equilibrium value from a small value is about 2.5 hr. It is much longer as compared with the characteristic time $(\tau\sim l/\sqrt{\bar{e}}\sim10^2 s)$ of developed turbulence. As far as this problem is concerned, the computed results may be incorrect. Apparently, this problem results from the model itself, as the model aims mainly at the description of the motion with large Reynold number.

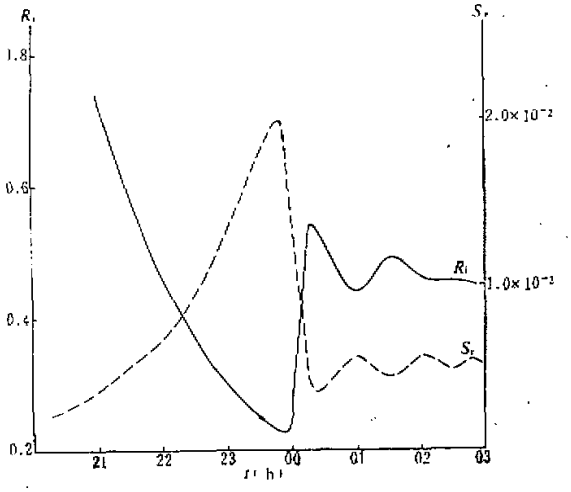

Fig. 7. The computed curves of intensity of wind shear S_v and Richardson number Ri in the layer where the sudden change first occurs.

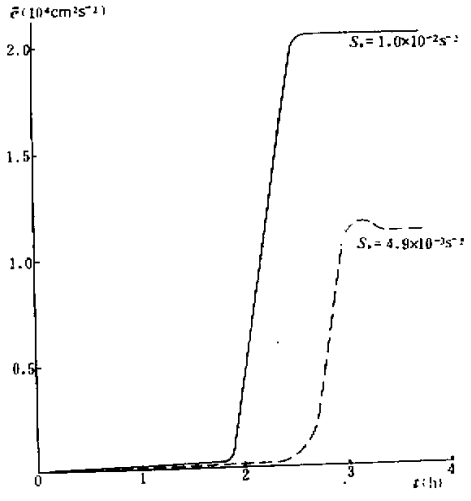

Fig. 8. The computed curves of the evolution of $\bar{e}$ at $Ri=0.3$ and different values of S_v.

The computed results also show that under the condition $Ri=0.5$, $\bar{e}$ always maintains small values of order 10^{-5} cm^2 s^{-2}. This is an indication that the turbulence no longer exists. Thus, the computed critic Richardson number Ri_c is about 0.5, whereas the Ri_c theoretically obtained for some kinds of motions is 0.25. Bush[20] (1972) pointed out that, in general, Ri_c is in the range of 0.25 to 0.5 in the lower atmosphere.

V. CONCLUSION

In this paper, a second-order model is set up for the description of stable boundary layer, and tested against the observed data. The results show that the computed main characteristics of wind and temperature are comparatively consistent with that observed in the NBL. Through analysing the results, we find that in order to simulate the evolution of the NBL fairly well one should simulate the wind accurately.

Also, a kind of sudden change is simulated. When the sudden change takes place, the second-order moments undergo great variation in a short time, later, they quasi-periodically change and decay in amplitude, and finally reach a stationary state. After the occurrence of the sudden change, the temperature falls considerably in the upper and middle parts, and rises in the lower part, of the inversion. The results show that the sudden change crops up when the Richardson number Ri gets a value below a critic value, Ri_c, decreasing from a larger value. In the real stable boundary layer, providing the local Ri falls to a value below Ri_c from larger values, the turbulence is to break out, it may stimulate the inner gravity-waves and with their spreading, they may in turn make certain stable layers unstable.

In the model, the diffusion effects of third-order moments on the second-order ones are neglected, thus the amplitude of sudden change may be overestimated.

REFERENCES

[1] Estoque, M., *J. Geophys. Res.*, **68**(1963), 1103—1113.
[2] Sasamori, T., *J. Atmos. Sci.*, **46**(1970). 137—154.
[3] Clarke, R.H., *Izv. Akad. Nauk SSSR, Fiz. Atmos. Okeana.*, **10**(1974), 600—612.
[4] Buajitti, K., and Blackadar, A.K., *Q.J.M.S.*, **83**(1957), 486—500.
[5] Paegle, J., and Rash, G.E., *Mon. Wea. Rev.*, **101**(1973), 746—756.
[6] Li Xingsheng et al., *Sci. Atmos. Sin.*, **6**(1980), 135—147.
[7] Yammada, T. et al., *J. Atmos. Sci.*, **27**(1975), 347—358.
[8] Wyngaard, J.C., *Bound-Layer Meteor.*, **9**(1975), 144—460.
[9] Andre, J.C. et al., *J. Atmos. Sci.*, **35**(1978), 1861—1883.
[10] Garret, J.R. and Brost, R.A., *J. Atmos. Sci.*, **38**(1981), 2730—2746.
[11] Rodgers, C.D., *Q.J.R.M.S.*, **93**(1967), 43—54.
[12] Launder, B.E., *J. Fluid Mech.*, **67**(1975), 569—581.
[13] Launder, B.E., *J. Fluid Mech.*, **68**(1975), 537—566.
[14] Wyngaard, J.C., and Cote, O.R., *J. Atmos. Sci.*, **28**(1971), 190—201.
[15] Twensend, A.A., *J. Fluid Mech.*, **4** (1958), 361—375.
[16] Brost, R.A., and Wyngaard, J.C., *J. Atmos. Sci.*, **35**(1978), 1427—1440.
[17] Clarke, R.H. et al., *The Wangara Experiment: Boundary Layer Data*, (1971), CSIRO, Melbourne, 1971.
[18] Blackadar, A.K., *Bull. Amer. Met. Soc.*, **38**(1957), 283—290.
[19] Zhou Mingyu et al., *A Monthly J. Sci.*, **3**(1982), 156—159.
[20] Bush, N.E., *Workshop on Micrometeorology*, Ed. D. A. Haugen, Amer. Met. Soc., 1972.